JOC The Journal of Organic Chemistry

Article

pubs.acs.org/joc

# DFT Mechanistic Study of Rh(III)-Catalyzed [3 + 2]/[5 + 2] Annulation of 4-Aryl-1,2,3-triazoles and Alkynes Unveils the Dual C−H Activation Strategy

Zhongchao Zhang, Shengwen Yang, Juan Li,* and Xiaojian Liao*

Department of Chemistry, Jinan University, Huangpu Road West 601, Guangzhou, Guangdong 510632, P. R. China

Supporting Information

**ABSTRACT:** Li and co-workers recently developed a dual C−H bond activation strategy, using a Rh(III) catalyst, for [3 + 2]/[5 + 2] annulation of primary 4-aryl-1,2,3-triazoles and alkynes. The Rh(III)-catalyzed dual annulation of 4-aryl-1,2,3-triazoles and alkynes is challenging because only single annulation is achieved using Rh(II) and Ni(0) catalysts. Intrigued by the novel strategy, we performed a density functional theory study to unravel this challenging dual C−H bond activation. A Friedel−Crafts type mechanism proved be more favorable than a concerted metalation−deprotonation (CMD) mechanism for the first C−H bond activation. The second C−H bond activation proceeded via a CMD mechanism. More importantly, the calculation explained why only $AgSbF_6$, among several candidates, performed perfectly, whereas others failed, and why the dual annulation of 4-aryl-1,2,3-triazoles with alkynes was achieved with a Rh(III) catalyst but not with Rh(II) and Ni(0) catalysts. Due to the active catalyst being $[Cp^*Rh(OAc)]^+$, $AgSbF_6$, in which $SbF_6^-$ is a stable anion, among several candidates performed perfectly. The success of the Rh(III)-catalyzed dual C−H bond activation has two origins: (i) the active catalyst $[Cp^*Rh(OAc)]^+$ is more stable than $Cp^*Rh(OAc)_2$ when the Ag salt is $AgSbF_6$, and this facilitates the first alkyne insertion; and (ii) a rhodium−carbene is easily formed.

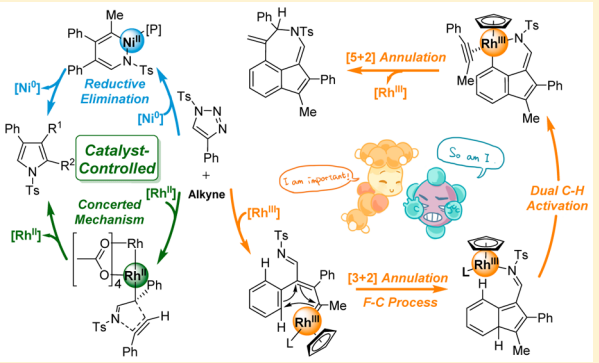


## 1. INTRODUCTION

Transition-metal-catalyzed cycloadditions provide a powerful tool for rapid, atom-economical construction of carbocyclic and heterocyclic compounds.[1] 1,2,3-Triazoles are important heterocyclic units with a broad range of biological activities and pharmacological properties.[2] The use of 1,2,3-triazoles as ideal precursors for constructing various heterocyclic molecules has attracted interest in recent years.[3,4] In this widely used synthetic strategy, metallocarbene intermediates are formed via 1,2,3-triazole ring opening in the presence of various transition-metal catalysts.

In particular, reactions involving $\pi$ components give access to more complex molecules.[5] Alkynes are often used as the $\pi$ component because of their wide range of reactivities in the presence of transition-metal catalysis.[6] However, they are seldom considered as $2\pi$ components in such transformations.[7] The annulation of 1,2,3-triazoles with alkynes is usually achieved by formal [3 + 2] or [4 + 2] cycloadditions to give five- or six-membered rings,[8] but the construction of larger rings using related annulations is rare.[9]

1,2,3-Triazoles can undergo metal-catalyzed [3 + 2] annulation with alkynes to produce pyrroles. In 2012, Murakami reported the Ni(0)/$AlPh_3$-catalyzed transannulation of *N*-tosyl-1,2,3-triazoles with internal alkynes to give tetrasubstituted pyrroles (Scheme 1).[8e] In addition to nickel(0)/phosphine catalyst, the binary catalyst $Rh_2(oct)_4$/$AgOCOCF_3$ was also reported to be effective to promote the annulation of *N*-tosyl-1,2,3-triazoles with terminal alkynes by Gevorgyan and co-workers (Scheme 1).[8b] The Rh(III)-catalyzed [3 + 2]/[5 + 2] annulation of 4-aryl-1,2,3-triazoles with alkynes was recently reported by Li's group (Scheme 2).[10]

**Scheme 1. Metal-Catalyzed [3 + 2] Annulation of *N*-Tosyl-1,2,3-triazoles with Alkynes**

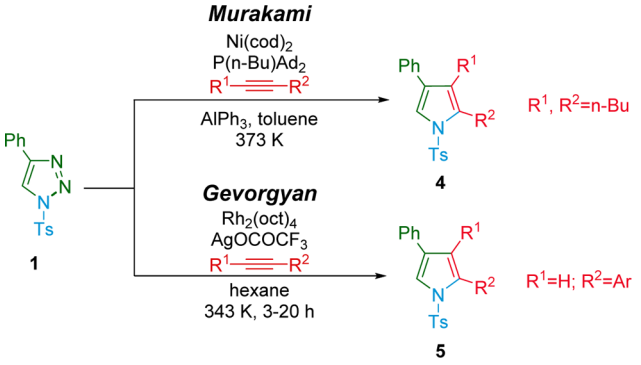


**Received:** July 15, 2016
**Published:** October 3, 2016





DOI: 10.1021/acs.joc.6b01706
J. Org. Chem. 2016, 81, 9639−9646

**Scheme 2. Rh(III)-Catalyzed [3 + 2]/[5 + 2] Annulation of 4-Aryl-1,2,3-triazoles with Alkynes**

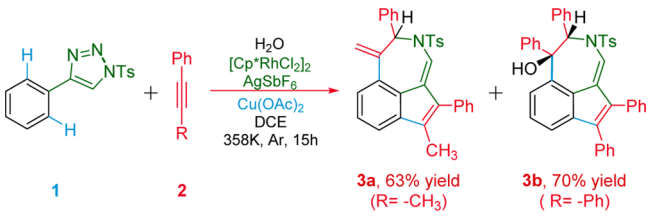


Y. Yang, M. B. Zhou, X. H. Ouyang, R. Pi, R. J. Song, J. H. Li
*Angew. Chem. Int. Ed.* **2015**, *54*, 6595

This is the first report of the metal-catalyzed [3 + 2]/[5 + 2] annulation of 4-aryl-1,2,3-triazoles through dual C($sp^2$)−H functionalization. The use of different substituents (e.g., Me and Ph) on the internal alkynes led to formation of either 1-methyleneindeno[1,7-*cd*]azepines **3a** or indeno[1,7-*cd*]azepin-1-ols **3b**.

The dual [3 + 2]/[5 + 2] annulation shown in Scheme 2 is important, but its mechanism is poorly understood. It is important to elucidate the detailed reaction mechanism, including the origins of the observed chemoselectivity. Remarkably, the dual annulation of 4-aryl-1,2,3-triazoles with alkynes can be achieved using a Rh(III) catalyst, but neither Rh(II) nor Ni(0) catalysts. We further question why Rh(III) can cause dual annulation of 1,2,3-triazoles. Li et al. examined several Ag salts, but only $AgSbF_6$ acted efficiently, and others delivered no product at all. This raises the following questions: why is $AgSbF_6$ unique, and how can effective Ag salts be identified? Computational studies could help to broaden the scope and patterns of Rh(III)-catalyzed dual C−H activation systems.

## 2. COMPUTATIONAL DETAILS

The molecular geometries of the complexes were optimized using density functional theory (DFT) calculations at the M06 level.[11] Frequency calculations were also performed at the same level of theory to identify all the stationary points as minima (zero imaginary frequencies) or transition states (one imaginary frequency), and the free energies at 298.15 K. An IRC[12] analysis was performed to confirm that all the stationary points were smoothly connected to each other. The Rh and S atoms in this analysis were described using the LANL2DZ basis set, including a double-valence basis set with the Hay and Wadt effective core potential.[13] Polarization functions were added for Rh ($\zeta_f$ = 1.350) and S ($\zeta_f$ = 0.503).[14] The 6-31+G*[15] basis set was used for the other atoms. Single-point energy calculations were conducted using the polarizable continuum model (PCM)[16] to evaluate the solvent effects for all the gas-phase optimized species. SDD[17] basis sets were used for the Rh atom in the PCM calculations, and the 6-311+G** basis set was used for all other atoms. The three-dimensional images of the optimized structures were prepared using CYLview.[18] All calculations were performed using the Gaussian 09 package.[19]

## 3. RESULTS AND DISCUSSION

In this study, we used 4-aryl-1,2,3-triazoles **1** with 1-phenyl-1-propyne **2** as a representative system (i.e., R = Me in Scheme 2) for clarifying the reaction mechanism and chemoselectivity.

**3.1. Role of Ag Salt.** In the reaction system, different Rh(III) species (such as Cp*$RhCl_2$, Cp*Rh(OAc)Cl, Cp*Rh-$(OAc)_2$, [Cp*Rh(OAc)]$^+$, and Cp*Rh(OAc) ($SbF_6$)) may exist in the presence of a precatalyst $[Cp^*RhCl_2]_2$, $AgSbF_6$ additive, and oxidant $Cu(OAc)_2$. Because the most stable of these Rh(III) species is [Cp*Rh(OAc)]$^+$ as shown in Table 1, it is reasonable to take [Cp*Rh(OAc)]$^+$ as the active catalyst (reference point, 0 kcal/mol). Li et al.[10] reported that the annulation of 4-aryl-1,2,3-triazoles with alkynes does not take place when AgOAc and AgOTf are used as the salt. This can be explained as follows. Relative to $[Cp^*RhCl_2]_2$, [Cp*Rh(OAc)]$^+$ is highly endergonic and unstable when AgOAc and AgOTf salts are used (Table 1), and this suppresses the subsequent reaction. The relative stability of [Cp*Rh(OAc)]$^+$ can be attributed to the stability of the anion in the Ag salt. $SbF_6^-$ is obviously the most stable of the three anions used, which makes [Cp*Rh(OAc)]$^+$ the most stable among all Rh(III) species. In contrast, all Rh(III) species are highly endergonic and unstable when AgOAc and AgOTf salts are used (Table 1), except Cp*$RhCl_2$ which is formed without the assistance of the Ag salt.

**3.2. Sequence of C−H Cleavage and Alkyne Insertion.** In calculations of reaction mechanism, a Cp was used instead of Cp* as the ligand to reduce the computational costs.[21] The first step in the dual annulation reaction is ring opening of the 4-aryl-1,2,3-triazole via N−N single-bond cleavage. The free energy of the ring-opening transition state **TS-1** was determined to be 22.3 kcal/mol. Ring opening of 1,2,3-triazoles in the presence of [CpRh(OAc)]$^+$ is less favorable (Scheme 3) in terms of activation free energies (23.9 kcal/mol). A catalyst-assisted ring-opening mechanism is therefore ruled out. Figure 1 shows that the transformation of **1** to **IN-1** is endergonic, which is consistent with the previous suggestion that there is a closed-/open-form equilibrium between 1,2,3-triazole and *α*-diazoimine species.[22] The subsequent coordination of [CpRh-(OAc)]$^+$ to **IN-1** leads to the formation of intermediate **IN-2**. The next step, i.e., $N_2$ liberation, occurs via transition state **TS-2** to give **IN-3**, with an energy barrier of 9.0 kcal/mol relative to **IN-1**.

From **IN-3**, either C−H cleavage or alkyne insertion could occur first. We performed calculations for the two pathways (black line for the first alkyne insertion and red line for the first C−H-bond-breaking step in Figure 1). For the first alkyne insertion, alkyne coordination to the Rh center gives **IN-4**, which is then converted to **IN-5** via alkyne insertion, with an energy barrier of 22.8 kcal/mol relative to **IN-3**. **IN-5** further rearranges to give the rhodium carbene **IN-6** (see Figure 2), which has a small energy barrier of 6.4 kcal/mol. In the first C−H-breaking pathway, a concerted metalation−deprotonation

**Table 1. Solvent-Phase Free Energy Profiles (kcal/mol) of Rh(III) Species Relative to Precatalyst $[Cp^*RhCl_2]_2$ with Different Ag Salts[20]**

| | | Cp*$RhCl_2$ | Cp*Rh(OAc)Cl | [Cp*Rh(OAc)]$^+$ | Cp*$Rh(OAc)_2$ | Cp*Rh(OAc)X |
|---|---|---|---|---|---|---|
| 1 | $AgSbF_6$ | −2.8 | 5.8 | −5.0 | 27.5 | 10.8 |
| 2 | AgOTf | −2.8 | 24.0 | 31.3 | 63.8 | 30.7 |
| 3 | AgOAc | −2.8 | 58.4 | 100.1 | 132.6 | 66.8[a] |

[a]X = $SbF_6^-$, $OTf^-$, or $OAc^-$ which derived from the silver salt.



DOI: 10.1021/acs.joc.6b01706
*J. Org. Chem.* 2016, 81, 9639−9646

**Scheme 3. Ring Opening of 1,2,3-Triazoles in the Presence of [CpRh(OAc)]$^+$**

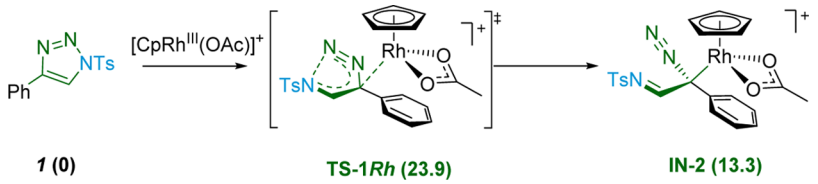


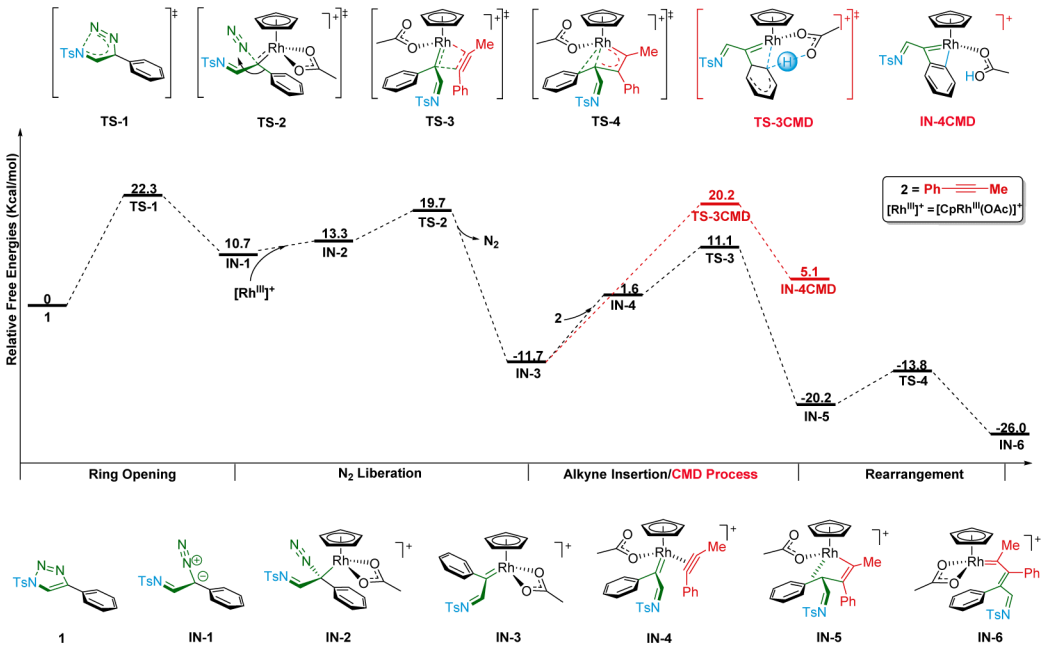


**Figure 1.** Calculated free energy profiles for key steps in first alkyne insertion (black line) and first C−H cleavage (red line) pathways. Solvent-corrected free energies in PCM model are given in kcal/mol.

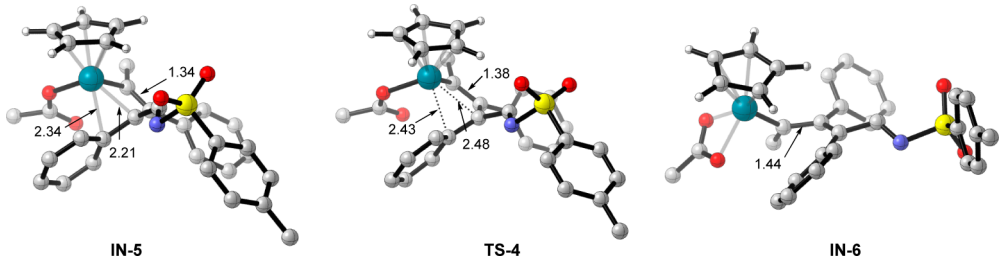


**Figure 2.** Optimized structures of **IN-5**, **TS-4**, and **IN-6** along with key bond lengths (in angstroms). Some hydrogen atoms have been omitted for clarity. Rh, C, O, N, and S atoms are shown in dark green, silver gray, red, blue, and yellow, respectively.

(CMD) mechanism, in which metal−carbon bond formation occurs concurrently with cleavage of the C−H arene bond, starts from **IN-3**. This step affords four-membered rhodacyclic species **IN-4CMD**, in which HOAc is still bound to Rh. The free energy of the CMD transition state **TS-3CMD** is calculated to be 20.2 kcal/mol, which is higher than that of **TS-3** (11.1 kcal/mol), for the first alkyne insertion pathway. The first C−H cleavage pathway is consequently ruled out; this can be explained as follows. The first C−H cleavage pathway would result in the formation of a highly unstable four-membered rhodium carbene ring, which would lead to a pronounced increase in the overall energy demand of the first C−H cleavage pathway.

**3.3. Friedel−Crafts Type or CMD Mechanism for First C−H Activation.** Continuing with the first [3 + 2] annulation pathway, the arene C−H activation will take place from the intermediate **IN-6**. In the Friedel−Crafts type mechanism[23] shown in Figure 3, the carbene attacks the phenyl moiety in a fashion similar to electrophilic aromatic substitution via **TS-5FC** (see Figure 4) to form **IN-7FC**, with a barrier of 5.5 kcal/mol. Another molecule of [CpRh(OAc)]$^+$ enters to form the divalent cation **IN-8FC**, and then the original [CpRh(OAc)]$^+$ dissociates to yield intermediate **IN-9FC**. Subsequent C−H deprotonation via **TS-6FC** (see Figure 4) reinstates the aromaticity of the benzene ring and generates the complex **IN-10FC** and then the [3 + 2] product **IN-11** through removal of a single molecule of neutral HOAc. For the CMD mechanism shown in Figure 3, the free energy of transition state **TS-5CMD** (−17.9 kcal/mol) for the CMD step is higher than that of **TS-6FC** (−20.5 kcal/mol) and is therefore ruled out. A CMD mechanism has been suggested for Rh(III)-catalyzed C−H activation based on recent DFT calculations.[24]



DOI: 10.1021/acs.joc.6b01706
J. Org. Chem. 2016, 81, 9639−9646

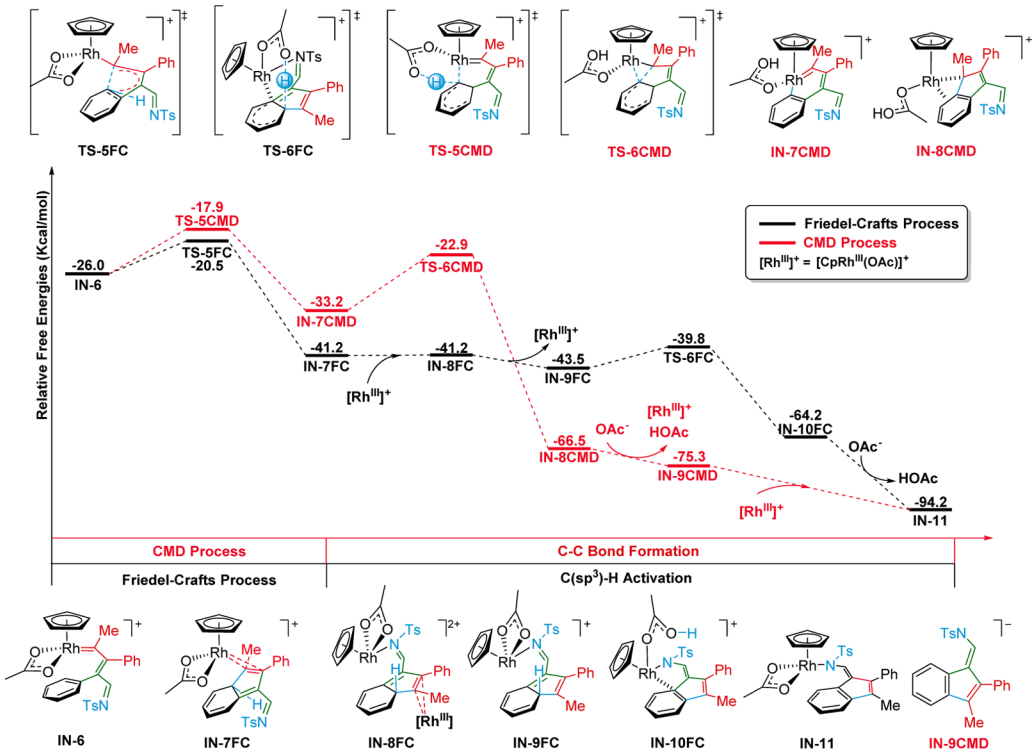


**Figure 3.** Calculated free energy profiles for processes **IN-6** → **IN-11** (black line for Friedel–Crafts mechanism and red line for CMD mechanism). Solvent-corrected free energies in PCM model are given in kcal/mol.

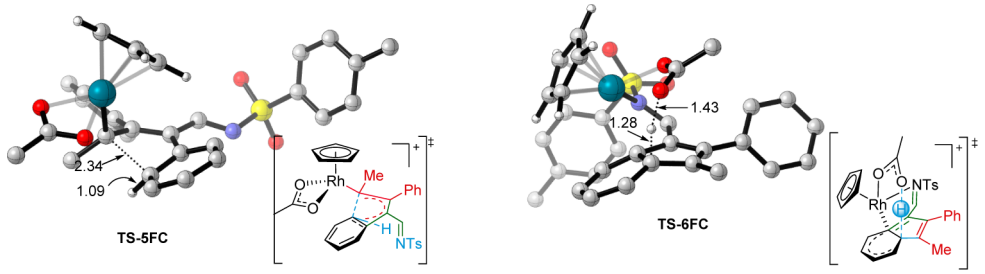


**Figure 4.** Optimized structures of **TS-5FC** and **TS-6FC** along with key bond lengths (in angstroms). Some hydrogen atoms have been omitted for clarity. Rh, C, O, N, and S atoms are shown in dark green, silver gray, red, blue, and yellow, respectively.

Our calculations show that a Friedel–Crafts type mechanism is more favorable than a CMD mechanism for this system. **TS-5FC** is more stable than **TS-5CMD** because the unstable rhodium carbene remains unchanged throughout the CMD mechanism but not in the Friedel–Crafts type mechanism.

**3.4. Second C–H Activation.** The second C–H activation starts from **IN-11** via a CMD mechanism. The Rh center in **IN-11** approaches the arene C–H bond, leading to **IN-11** featuring a C–H bond anagostic coordination to the Rh(III) center with an elongated C–H bond length (1.10 Å). The formation of **IN-13** holds an activation energy barrier of 14.0 kcal/mol. **IN-13** further undergoes dissociation of HOAc and coordination of the alkyne, which leads to 18*e* Rh(III) complex **IN-14**. The alkyne then inserts into the Rh(III)–C bond by spanning a barrier of 13.9 kcal/mol (**TS-8**) relative to **IN-13**, generating **IN-15**. Subsequently, **IN-15** approaches the carbon atom linked to the methyl group and is converted to **IN-16**. Rh(III) **IN-16** then undergoes reductive elimination, with C–N bond formation, to give Rh(I) **IN-17**, overcoming a low barrier of 6.2 kcal/mol (**TS-9**).

An alternative pathway from **IN-15** was also considered as shown in Figure 5 (red line), in which migration of a proton from HOAc to the phenyl-group-bonded carbon occurs prior to the C–N-bond-forming reductive elimination. However, the energy barrier for the alternative process, i.e., **IN-15** → **IN-17ByPro**, is 20.9 kcal/mol, which is 9.7 kcal/mol higher than that for **IN-15** → **IN-17**. Compared to **IN-15** → **IN-17ByPro**, the reason for the low activation barrier of **IN-15** → **IN-17** should be attributed to the conjugation becoming strong as the C–N bond formation proceeds. This result is consistent with the experimental findings[10] that the seven-membered ring is not formed directly by nucleophilic addition of the N–H bond to the alkene. Li et al.[10] reported that 14% of the byproduct, which was formed through the phenyl-group-bonded carbon occurred prior to the C–N-bond-forming reductive elimination, was obtained when cyclopropyl acetylene was the substrate. Our calculations (Figure 5) show that the energy difference between the two processes for the 1-phenyl-1-propyne substrate (**IN-15** → **IN-17** and **IN-15** → **IN-17ByPro**) is 9.7 kcal/mol, whereas the difference for the cyclopropylacetylene substrate is 5.8 kcal/mol.[25] The lower


DOI: 10.1021/acs.joc.6b01706
J. Org. Chem. 2016, 81, 9639–9646

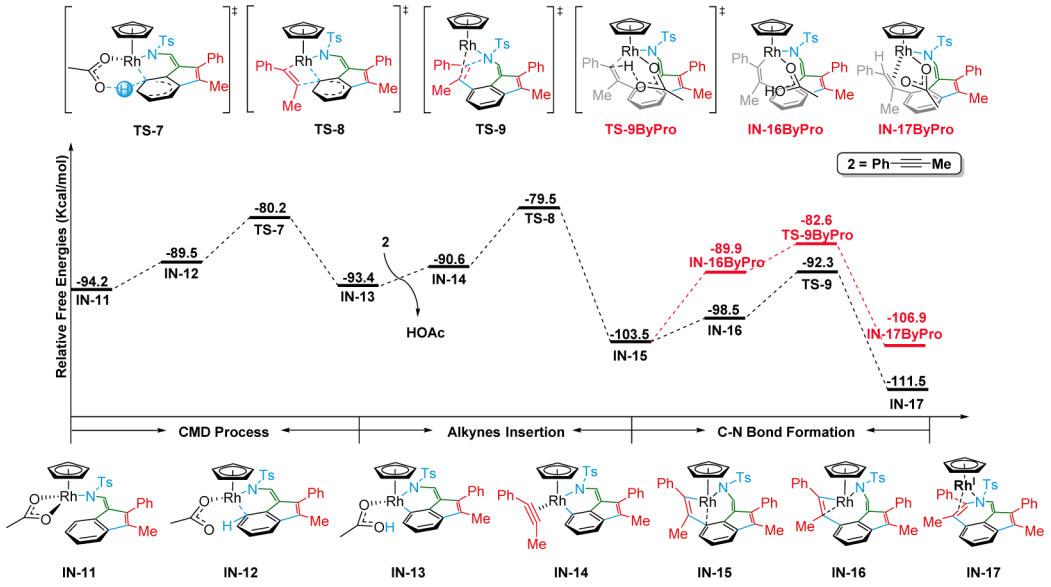


**Figure 5.** Calculated free energy profiles for processes **IN-11** → **IN-17** (black line) and **IN-11** → **IN-17ByPro** (red line). Solvent-corrected free energies in PCM model are given in kcal/mol.

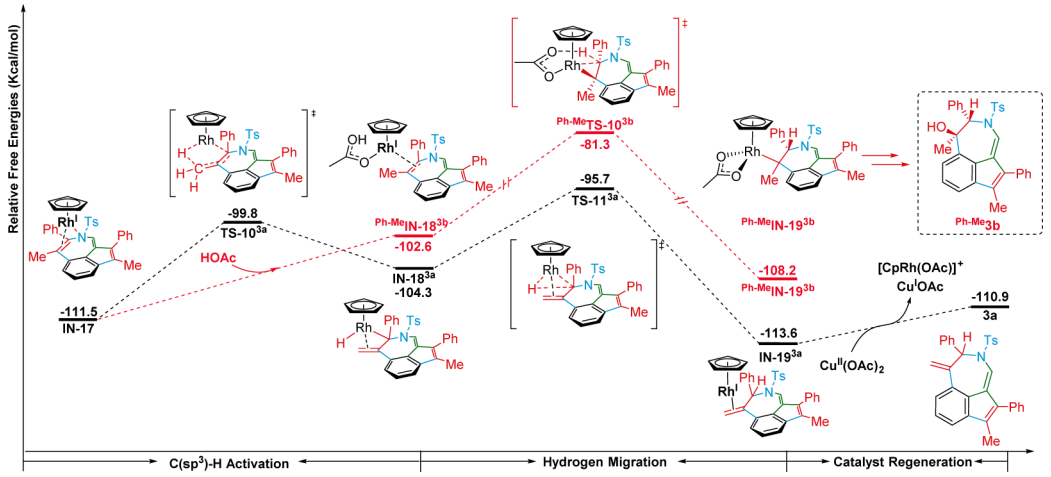


**Figure 6.** Calculated free energy profiles for processes **IN-17** → **3a** (black line) and **IN-17** → $^{Ph-Me}$**IN-19**$^{3b}$ (red line). Solvent-corrected free energies in PCM model are given in kcal/mol.

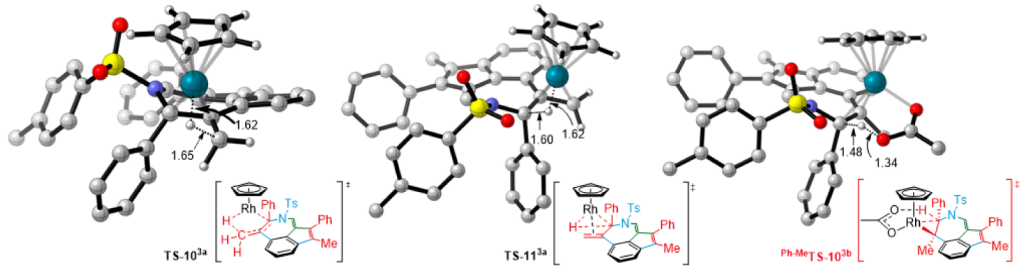


**Figure 7.** Optimized structures of **TS-10**$^{3a}$, **TS-11**$^{3a}$, and $^{Ph-Me}$**TS-10**$^{3b}$, along with key bond lengths (in angstroms). Some hydrogen atoms have been omitted for clarity. Rh, C, O, N, and S atoms are shown in dark green, silver gray, red, blue, and yellow, respectively.

energy difference for the cyclopropylacetylene system leads to byproduct formation.

**3.5. Origin of Chemoselectivity.** Figure 6 shows that **IN-17** determines whether the final product is **3a** or $^{Ph-Me}$**3b**. In the straightforward pathway to **3a** (black line in Figure 6), the Rh(I) complex **IN-17** is oxidized to the Rh(III)−hydrogen complex **IN-18**$^{3a}$ by oxidative addition via transition state **TS-10**$^{3a}$ (see Figure 7). Hydrogen then migrates to the phenyl-group-bonded nitrogen atom via transition state **TS-11**$^{3a}$ (see Figure 7), generating the stable (−113.6 kcal/mol) 16e Rh(I) $\pi$ complex **IN-19**$^{3a}$. Finally, the catalyst is regenerated via oxidation of $Cu(OAc)_2$ with concomitant release of the desired product **3a**. If the overall process of formation of **3a** (Figures 1, 3, 5, and 6) is taken into consideration, the rate-determining



DOI: 10.1021/acs.joc.6b01706
J. Org. Chem. 2016, 81, 9639−9646

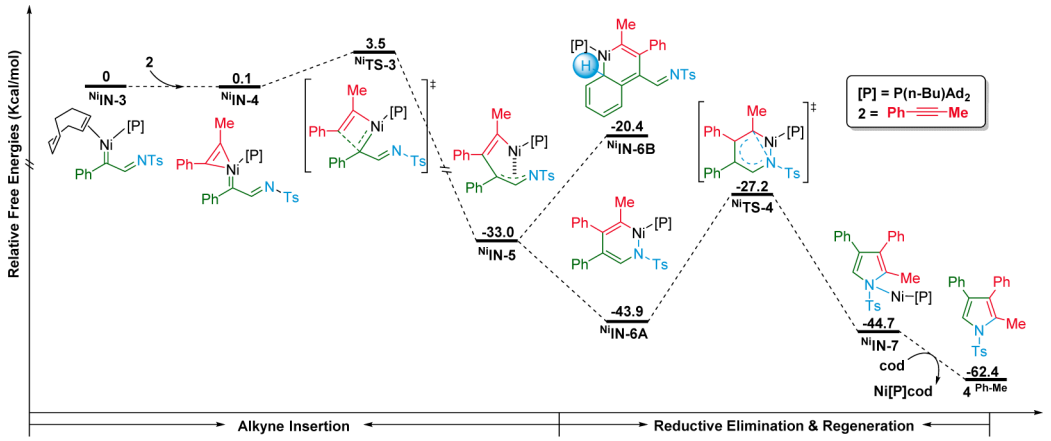


**Figure 8.** Calculated free energy profiles for Ni(0)-catalyzed processes $^{Ni}$**IN-3** → **4**. Solvent-corrected free energies in PCM model are given in kcal/mol.

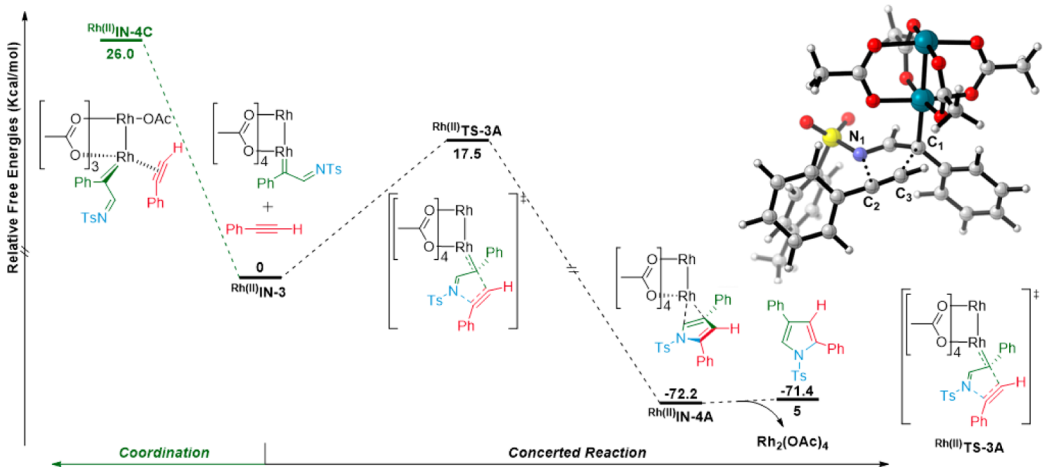


**Figure 9.** Calculated free energy profiles for Rh(II)-mediated processes $^{Rh(II)}$**IN-3** → **5**. Solvent-corrected free energies in PCM model are given in kcal/mol.

step is the first alkyne insertion, with an energy barrier of 22.8 kcal/mol.

In the pathway to $^{Ph-Me}$**3b** (Figure 6, red line), HOAc coordinates to **IN-17** to form the 18e Rh(I) complex $^{Ph-Me}$**IN-18**[3b]. HOAc then assists protonation of the carbon atom linked to the −NTs moiety via transition state $^{Ph-Me}$**TS-10**[3b] (see Figure 7) by spanning a barrier of 30.2 kcal/mol, leading to Rh(III) complex $^{Ph-Me}$**IN-19**[3b]. Because the protonation barrier, i.e., 30.2 kcal/mol, is much higher than that for the formation of **3a** (15.8 kcal/mol), the pathway to the resulting product $^{Ph-Me}$**3b** is less kinetically favorable. The instability of $^{Ph-Me}$**TS-10**[3b] compared with **TS-11**[3a] can be attributed to the relatively high oxidation state Rh(III).

**3.6. Why Rh(III) Catalyst Exhibit Dual Annulation?** As discussed in the Introduction, the dual annulation of 4-aryl-1,2,3-triazoles with alkynes occurs only with a Rh(III) catalyst, and not with Rh(II) and Ni(0) catalysts. In this section, we explain how Rh(III) can achieve dual annulation of 1,2,3-triazoles. Figure 1 shows that formation of the rhodium carbene **IN-6** plays a key role in dual annulation. To understand single annulation with Rh(II) and Ni(0), and to corroborate our proposed mechanism for the Rh(III) system, we replaced Rh(III) with Ni(0) or Rh(II) and computed the pathways for annulation of 4-aryl-1,2,3-triazoles with alkynes. The detailed results are given in Figures 8 and 9. We used $^{Ni}$**IN-3** and $^{Rh(II)}$**IN-3** as energy references for constructing the energy profile because ring opening of 4-aryl-1,2,3-triazoles and $N_2$ liberation do not affect single or dual annulation of 1,2,3-triazoles. For the Ni(0) system, alkyne insertion is facile because the Ni center is unsaturated, and the energy barrier is only 3.4 kcal/mol ($^{Ni}$**TS-3** relative to $^{Ni}$**IN-4**). Alkyne insertion gives $^{Ni}$**IN-5**, which can then undergo rearrangement. Because Ni is a first-row late-transition metal, its d orbitals are contracted; therefore, $^{Ni}$**IN-5** is not transformed into nickel carbene similarly to **IN-6** in the Rh(III) system. $^{Ni}$**IN-6A** and $^{Ni}$**IN-6B** are two possible ensuing intermediates. Dual annulation could proceed from $^{Ni}$**IN-6B**, and single annulation could proceed from $^{Ni}$**IN-6A**. $^{Ni}$**IN-6A** is 23.5 kcal/mol more stable than $^{Ni}$**IN-6B**; this notably implies that the transformation tends to undergo single annulation via $^{Ni}$**TS-4**.

We used $Rh_2(OAc)_4$ instead of $Rh_2(oct)_4$ as a model catalyst in the calculations, to reduce the computational costs. Figure 9 shows a schematic diagram of the energetics using **1** and $Rh_2(OAc)_4$. If the alkyne insertion mode is similar to those in the Rh(III) and NI(0) systems, the Rh(II)−alkyne species $^{Rh(II)}$**IN-4C** is very unstable, with a free energy of 26.0 kcal/mol, because the high stability of $Rh_2(OAc)_4$ disfavors alkyne coordination to the Rh(II) center via ligand exchange. Alkyne connection to rhodium carbene through a concerted transition state $^{Rh(II)}$**TS-3A**, with simultaneous formation of C1−C3 and



DOI: 10.1021/acs.joc.6b01706
J. Org. Chem. 2016, 81, 9639−9646

C2−N1 bonds, is more reasonable. The $^{Rh(II)}$**TS-3A** has an energy barrier of 17.5 kcal/mol and gives the Rh-associated five-membered ring $^{Rh(II)}$**IN-4A**.

## CONCLUSIONS

A novel strategy based on dual C($sp^2$)−H functionalization of 4-aryl-1,2,3-triazoles to build indeno[1,7-*cd*]azepine structures was recently developed by Li et al. To facilitate extension of this strategy, we performed a DFT mechanistic study to clarify how Rh(III) catalyzes the [3 + 2]/[5 + 2] annulation of 4-aryl-1,2,3-triazoles with alkynes and why dual annulation occurs exclusively with a Rh(III) catalyst. The active catalyst was identified as $[Cp^*Rh(OAc)]^+$ rather than $[Cp^*Rh(OAc)_2]$.

A rhodium(III) carbene intermediate is first formed by ring opening of the 4-aryl-1,2,3-triazole and $N_2$ liberation. The [3 + 2] annulation is then achieved through alkyne insertion via a Friedel−Crafts type mechanism. The second C−H activation involves a CMD mechanism, followed by a second alkyne insertion. C−N-bond-forming reductive elimination further achieves [5 + 2] annulation. The origin of the chemoselectivity can be attributed to stepwise C($sp^3$)−H activation of the methyl group being more favorable than protonation of the carbon atom linked to the −NTs moiety. A nickel−carbene intermediate cannot be formed in the Ni(0) system, which is why single annulation occurs. The concerted alkyne insertion mode is more favorable for the Rh(II) system and induces single annulation.

## ASSOCIATED CONTENT

### Supporting Information

The Supporting Information is available free of charge on the ACS Publications website at DOI: 10.1021/acs.joc.6b01706.

Complete ref 19, calculated imaginary frequencies of all transition states species, and tables of Cartesian coordinates and electronic energies for all of the calculated structures (PDF)

## AUTHOR INFORMATION


### Corresponding Authors

*E-mail: tchjli@jnu.edu.cn (J.L.).
*E-mail: tliaoxj@jnu.edu.cn (X.L.).


### Notes

The authors declare no competing financial interest.

## ACKNOWLEDGMENTS

This work was supported by the National Natural Science Foundation of China (Grant No. 21573095), the Fundamental Research Funds for the Central Universities (Grant No. 21615405) and the high-performance computing platform of Jinan University.

## REFERENCES


(1) For selected reviews, see: (a) Campolo, D.; Gastaldi, S.; Roussel, C.; Bertrand, M. P.; Nechab, M. *Chem. Soc. Rev.* **2013**, *42*, 8434. (b) Pellissier, H.; Clavier, H. *Chem. Rev.* **2014**, *114*, 2775. (c) Weding, N.; Hapke, M. *Chem. Soc. Rev.* **2011**, *40*, 4525. (d) Amatore, M.; Aubert, C. *Eur. J. Org. Chem.* **2015**, *2015*, 265. (e) Tanaka, K.; Tajima, Y. *Eur. J. Org. Chem.* **2012**, *2012*, 3715. (f) Jiao, L.; Yu, Z.-X. *J. Org. Chem.* **2013**, *78*, 6842. (g) Inglesby, P. A.; Evans, P. A. *Chem. Soc. Rev.* **2010**, *39*, 2791. (h) Aubert, C.; Fensterbank, L.; Garcia, P.; Malacria, M.; Simonneau, A. *Chem. Rev.* **2011**, *111*, 1954. (i) Yamamoto, Y. *Chem. Rev.* **2012**, *112*, 4736.

(2) (a) Bourne, Y.; Kolb, H. C.; Radic, Z.; Sharpless, K. B.; Taylor, P.; Marchot, P. *Proc. Natl. Acad. Sci. U. S. A.* **2004**, *101*, 1449. (b) Whiting, M.; Muldoon, J.; Lin, Y. C.; Silverman, S. M.; Lindstrom, W.; Olson, A. J.; Kolb, H. C.; Finn, M. G.; Sharpless, K. B.; Elder, J. H.; Fokin, V. V. *Angew. Chem., Int. Ed.* **2006**, *45*, 1435. (c) Pande, V.; Ramos, M. J. *Bioorg. Med. Chem. Lett.* **2005**, *15*, 5129. (d) Holla, B. S.; Mahalinga, M.; Karthikeyan, M. S.; Poojary, B.; Akberali, P. M.; Kumari, N. S. *Eur. J. Med. Chem.* **2005**, *40*, 1173. (e) Lewis, W. G.; Green, L. G.; Grynszpan, F.; Radic, Z.; Carlier, P. R.; Taylor, P.; Finn, M. G.; Sharpless, K. B. *Angew. Chem., Int. Ed.* **2002**, *41*, 1053. (f) Amblard, F.; Cho, J. H.; Schinazi, R. F. *Chem. Rev.* **2009**, *109*, 4207. (g) Le Droumaguet, C.; Wang, C.; Wang, Q. *Chem. Soc. Rev.* **2010**, *39*, 1233−1239. (h) Thirumurugan, P.; Matosiuk, D.; Jozwiak, K. *Chem. Rev.* **2013**, *113*, 4905.

(3) For reviews, see: (a) Chattopadhyay, B.; Gevorgyan, V. *Angew. Chem.* **2012**, *124*, 886. (b) Gulevich, A. V.; Gevorgyan, V. *Angew. Chem.* **2013**, *125*, 1411. (c) Davies, H. M. L.; Alford, J. S. *Chem. Soc. Rev.* **2014**, *43*, 5151.

(4) For selected examples, see: (a) Ma, X.; Wu, F.; Yi, X.; Wang, H.; Chen, W. *Chem. Commun.* **2015**, *51*, 6862. (b) Lee, E.; Ryu, T. E.; Shin, S.; Choi, W.; Lee, P. *Org. Lett.* **2015**, *17*, 2470. (c) Chuprakov, S.; Worrell, B. T.; Selander, N.; Sit, R.; Fokin, V. V. *J. Am. Chem. Soc.* **2014**, *136*, 195. (d) Chen, K.; Zhu, Z.; Zhang, Y.; Tang, X.; Shi, M. *Angew. Chem., Int. Ed.* **2014**, *53*, 6645. (e) Parr, B.; Green, S.; Davies, H. M. L. *J. Am. Chem. Soc.* **2013**, *135*, 4716. (f) Schultz, E.; Sarpong, R. *J. Am. Chem. Soc.* **2013**, *135*, 4696.

(5) For reviews, see: (a) Patureau, F. W.; Wencel-Delord, J.; Glorius, F. *Aldrichimica Acta* **2012**, *45*, 31. (b) Hu, F.; Xia, Y.; Ma, C.; Zhang, Y.; Wang, J. *Chem. Commun.* **2015**, *51*, 7986.

(6) For selected examples, see: (a) Xu, T.; Ko, H. M.; Savage, N. A.; Dong, G. *J. Am. Chem. Soc.* **2012**, *134*, 20005. (b) Dreis, A. M.; Douglas, C. J. *J. Am. Chem. Soc.* **2009**, *131*, 412. (c) Kondo, T.; Kaneko, Y.; Taguchi, Y.; Nakamura, A.; Okada, T.; Shiotsuki, M.; Ura, Y.; Wada, K.; Mitsudo, T. *J. Am. Chem. Soc.* **2002**, *124*, 6824. (d) Shaw, M. H.; Melikhova, E. Y.; Kloer, D. P.; Whittingham, W. G.; Bower, J. F. *J. Am. Chem. Soc.* **2013**, *135*, 4992−4995.

(7) (a) Zhao, J.; Asao, N.; Yamamoto, Y.; Jin, T. N. *J. Am. Chem. Soc.* **2014**, *136*, 9540. (b) Anand, M.; Sunoj, R. B. *Org. Lett.* **2012**, *14*, 4584.

(8) (a) Shi, Y.; Gevorgyan, V. *Org. Lett.* **2013**, *15*, 5394. (b) Chattopadhyay, B.; Gevorgyan, V. *Org. Lett.* **2011**, *13*, 3746. (c) Alford, J. S.; Spangler, J. E.; Davies, H. M. L. *J. Am. Chem. Soc.* **2013**, *135*, 11712. (d) Xing, Y. P.; Sheng, G. R.; Wang, J.; Lu, P.; Wang, Y. G. *Org. Lett.* **2014**, *16*, 1244. (e) Miura, T.; Yamauchi, M.; Murakami, M. *Chem. Commun.* **2009**, 1470.

(9) Lee, D. J.; Han, H. S.; Shin, J.; Yoo, E. J. *J. Am. Chem. Soc.* **2014**, *136*, 11606.

(10) Yang, Y.; Zhou, M. B.; Ouyang, X. H.; Pi, R.; Song, R. J.; Li, J. H. *Angew. Chem., Int. Ed.* **2015**, *54*, 6595.

(11) (a) Zhao, Y.; Schultz, N. E.; Truhlar, D. G. *J. Chem. Phys.* **2005**, *123*, 161103. (b) Zhao, Y.; Truhlar, D. G. *Acc. Chem. Res.* **2008**, *41*, 157. (c) Zhao, Y.; Truhlar, D. G. *Theor. Chem. Acc.* **2008**, *120*, 215. (d) Zhao, Y.; Truhlar, D. G. *J. Chem. Theory Comput.* **2009**, *5*, 324.

(12) (a) Fukui, K. *J. Phys. Chem.* **1970**, *74*, 4161. (b) Fukui, K. *Acc. Chem. Res.* **1981**, *14*, 363.

(13) (a) Hay, P. J.; Wadt, W. R. *J. Chem. Phys.* **1985**, *82*, 299. (b) Wadt, W. R.; Hay, P. J. *J. Chem. Phys.* **1985**, *82*, 284.

(14) Ehlers, A. W.; Böhme, M.; Dapprich, S.; Gobbi, A.; Höllwarth, A.; Jonas, V.; Köhler, K. F.; Stegmann, R.; Veldkamp, A.; Frenking, G. *Chem. Phys. Lett.* **1993**, *208*, 111.

(15) Hariharan, P. C.; Pople, J. A. *Theor. Chim. Acta.* **1973**, *28*, 213.

(16) (a) Barone, V.; Cossi, M. *J. Phys. Chem. A* **1998**, *102*, 1995. (b) Cossi, M.; Rega, N.; Scalmani, G.; Barone, V. *J. Comput. Chem.* **2003**, *24*, 669. (c) Tomasi, J.; Mennucci, B.; Cammi, R. *Chem. Rev.* **2005**, *105*, 2999.

(17) (a) Fuentealba, P.; Preuss, H.; Stoll, H.; Vonszentpaly, L. *Chem. Phys. Lett.* **1982**, *89*, 418. (b) von Szentpaly, L.; Fuentealba, P.; Preuss, H.; Stoll, H. *Chem. Phys. Lett.* **1982**, *93*, 555. (c) Fuentealba, P.; Stoll, H.; Szentpaly, L. V.; Schwerdtfeger, P.; Preuss, H. *J. Phys. B: At. Mol. Phys.* **1983**, *16*, L323.




DOI: 10.1021/acs.joc.6b01706
*J. Org. Chem.* 2016, 81, 9639−9646

(18) Legault, C. Y. *CYLview*, 1.0b; Universite de Sherbrooke: 2009. http://www.cylview.org.
(19) Frisch, M. J. *Gaussian 09*, revision C.01; Gaussian, Inc: Wallingford, CT, 2010 [full reference given in Supporting Information].
(20) More details are given in Table S2 in the Supporting Information.
(21) One may question whether the electronic and steric effects on the reaction mechanism of Cp* are well modeled. We did a testing calculation using Cp* for the key transition states **TS-5CMD** and **TS-5FC**. See Figure S4 in the Supporting Information.
(22) (a) Hermes, M. E.; Marsh, F. D. *J. Am. Chem. Soc.* **1967**, *89*, 4760. (b) Harmon, R. E.; Stanley, J. F.; Gupta, S. K.; Johnson, J. *J. Org. Chem.* **1970**, *35*, 3444.
(23) For selected examples of the Friedel−Crafts type mechanism, see: (a) Arockiam, P. B.; Bruneau, C.; Dixneuf, P. H. *Chem. Rev.* **2012**, *112*, 5879. (b) Sandtorv, A. H. *Adv. Synth. Catal.* **2015**, *357*, 2403 and references cited therein.
(24) (a) Xu, L.; Zhu, Q.; Huang, G.; Cheng, B.; Xia, Y. *J. Org. Chem.* **2012**, *77*, 3017. (b) Guo, W.; Zhou, T.; Xia, Y. *Organometallics* **2015**, *34*, 3012. (c) Zhou, T.; Guo, W.; Xia, Y. *Chem. - Eur. J.* **2015**, *21*, 9209. (d) Guo, W.; Xia, Y. *J. Org. Chem.* **2015**, *80*, 8113. (e) Li, J.; Qiu, Z. *J. Org. Chem.* **2015**, *80*, 10686. (f) Du, L.; Xu, Y.; Yang, S.; Li, J.; Fu, X. *J. Org. Chem.* **2016**, *81*, 1921.
(25) See Scheme S1 and Figures S1 and S2 in the Supporting Information for details.



DOI: 10.1021/acs.joc.6b01706
*J. Org. Chem.* 2016, 81, 9639−9646